ACS OMEGA

http://pubs.acs.org/journal/acsodf

Article

Synthesis of Ag−Cu−Ni Nanoparticles Stabilized on Functionalized g−C_3N_4 and Investigation of Its Catalytic Activity in the A^3-Coupling Reaction

Mohammad Zarei, Iman Mohammadzadeh, Kazem Saidi, and Hassan Sheibani*

Cite This: *ACS Omega* 2023, 8, 18685−18694

Read Online

ACCESS | Metrics & More | Article Recommendations | Supporting Information

ABSTRACT: In the present research, using ethylenediamine and hydrazine hydrate as the capping and reducing agents in this investigation, respectively, Ag−Cu−Ni NPs were immobilized on the functionalized g−C_3N_4 surface. This nanocatalyst was studied in terms of its catalytic activities for the A^3-coupling reaction to synthesize propargylamine derivatives. According to the results, in the presence of 1 mL of toluene as the solvent and 20 mg of the g−C_3N_4−TCT−2AEDSEA−Ag−Cu−Ni nanocatalyst, the maximum efficiency of the nanocatalyst occurred at a temperature of 80 °C. Products were purified using thin-layer chromatography plates (silica gel) by employing *n*-hexane/ethyl acetate with a 90:10 ratio. In addition, the prominent benefits of the synthesized nanocatalyst include its high yields of the product, cost-effectiveness, recyclability, and easy separation. The novelty of the catalyst is due to the presence of Ag−Cu−Ni nanoparticles at the same time in the structure of the functionalized g−C_3N_4 substrate. So, Ag−Cu−Ni can be strongly connected to the substrate. The structure of the synthesized nanocatalyst was characterized using Fourier transformed infrared spectroscopy, X-ray powder diffraction, field emission scanning electron microscopy, energy-dispersive X-ray spectroscopy, vibrating-sample magnetometry, and transmission electron microscopy.

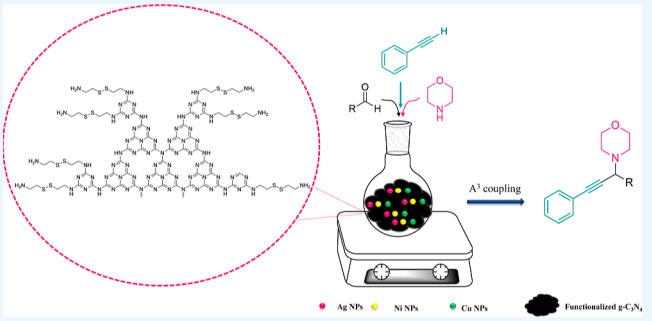

1. INTRODUCTION

In the current age, the synthesis of preparing efficient chemical compounds and biologically active molecules is a consideration via the use of nonhazardous metals.[1,2] Multi-component reactions (MCRs) play a crucial role in the synthesis of complex and new molecules. These reactions have attracted a significant deal of attention in the field of hybrid chemistry due to their artificial efficiency, inherent atomic economy, high selectivity, and simple procedure. Different MCRs, such as the Biginelli reaction, the Mannich reaction, and the Ugi reaction, have found extensive applications in the synthesis of various compounds using three or four primary materials.[3−8] One of the well-known MCRs is the A^3 reaction.[9] The A^3-coupling reaction is a three-component reaction via C−N and C−C couplings.[10,11]

Propargylamines are useful intermediates and have found wide applications in the synthesis of organic compounds for the construction of different nitrogen-containing heterocycles.[12,13] Propargylamines are one of the precursors used in organic chemistry. Countless propargylamines have been utilized to treat neurodegenerative disorders such as Alzheimer's and Parkinson's. Moreover, natural components are the key intermediates in the synthesis of biologically active drugs and products. These compounds are synthesized using A^3-coupling reaction.[14−16] So far, various catalysts such as Cu salt,[17] Au salt,[18] Ag salt,[19] Zn salt, Fe salt,[20] and iridium complexes[21] have been used for the synthesis of propargylamine derivatives in homogeneous conditions. The use of recyclable heterogeneous catalysts and inexpensive metals in this method is of great importance.[22−25] Metal nanoparticles have attracted attention of researchers due to their high surface-to-volume ratio and highly active surface. Among metal NPs, silver, nickel, and copper have been widely used due to their availability and high catalytic efficiency. Three metallic nanoparticles have attracted more attention than monometallic nanoparticles due to their synergistic effect. One of the main problems of the usage of nanoparticles in reactions is associated with their aggregation. Stabilization of nanoparticles on appropriate supports overcomes their stability problem. Different supports have been used for the stabilization of nanoparticles such as zeolite, TiO_2, graphene oxide, carbon-based supports, and Fe_3O_4. Among the various supports, g−C_3N_4 has exhibited good chemical resistance due to the incorporation of nitrogen atoms in the carbon structure that can result in enhancement of its chemical,

Received: January 28, 2023
Accepted: April 12, 2023
Published: May 15, 2023

Scheme 1. Synthesis of g−C_3N_4−TCT−2AEDSEA

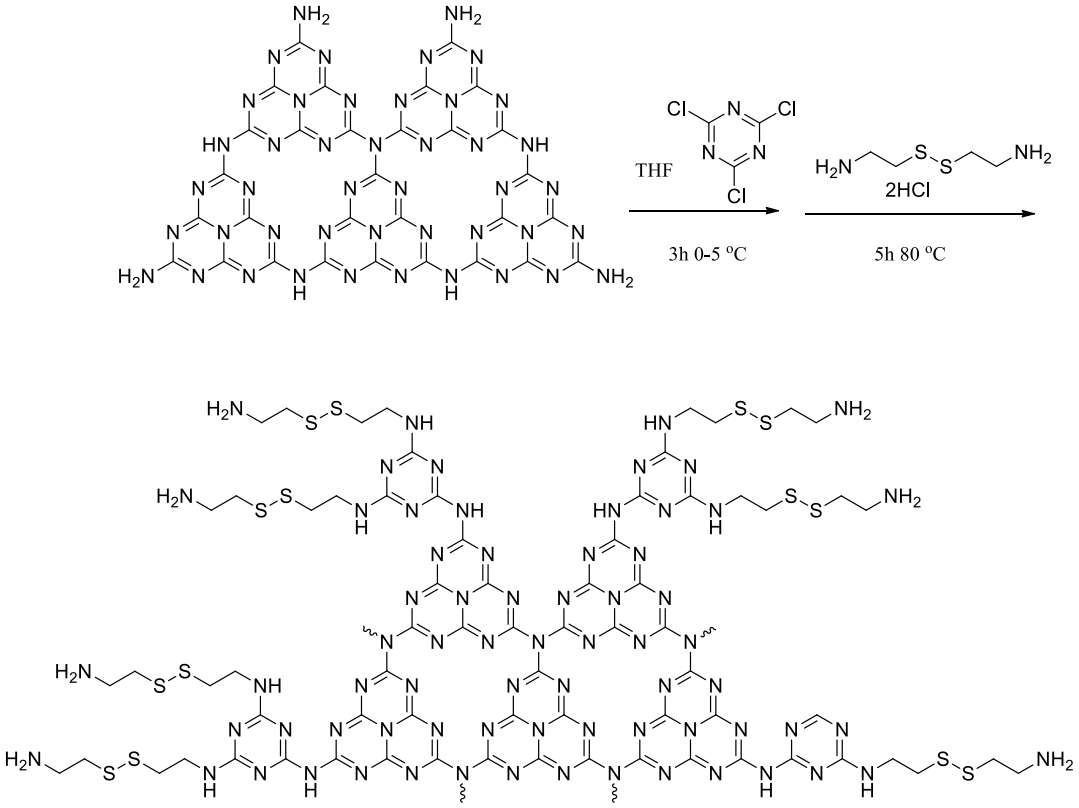

catalytic, electrical, and optical properties. To enhance the number of active sites of g−C_3N_4, it has been functionalized by melamine and cystamine dihydrochloride. Then, Ag−Cu−Ni NPs were placed on the surface of functionalized g−C_3N_4. The reactivity nanocomposite was then investigated in the one-pot reaction of secondary amines, terminal alkynes, and aldehydes for the preparation of propargylamines (A^3-coupling reaction). This project's purpose is to prepare propargylamine derivatives using a reasonable, straightforward, and economically suitable method.

2. EXPERIMENTAL SECTION

2.1. Materials and Chemical Instruments. Nickel (II) chloride ($NiCl_2{\cdot}6H_2O$), copper (II) chloride ($CuCl_2{\cdot}2H_2O$), Silver nitrate ($AgNO_3$), ethylenediamine (C_2H_4 $(NH_2)_2$), cystamine dihydrochloride ($C_4H_{14}Cl_2N_2S_2$), and cyanuric chloride ($C_3Cl_3N_3$) were obtained from Merck and Aldrich Chemical Companies and were used without further purification. The NMR spectra were recorded on a Bruker 300 AVANCE III NMR magnet (300 MHz for ^{1}H NMR and 75 MHz for ^{13}C NMR) using $CDCl_3$ as a solvent. The crystalline structure was investigated using an X-ray diffractometer (Phillips PANalytical X'Pert PRO with Cu Kα radiation λ = 0.154 nm), scanning electron microscopy images, EDX analyses (MIRA III device manufactured by TE-SCAN), and magnetic vibration diagrams [vibrating-sample magnetometry (VSM), magnetic Kavir Kashan Co., Iran].

2.2. Preparation Steps of the g−C_3N_4−TCT−2AEDSEA−Ag−Cu−Ni Nanocomposite. *2.2.1. Synthesis of g−C_3N_4.* The g−C_3N_4 powder was synthesized by polymerization of melamine.[26] In brief, 10.0 g of melamine powder in a ceramic crucible was placed in a muffle furnace at 550 °C for 4 h. The product was then transferred to a desiccator for about 2 h.

2.2.2. Preparation of g−C_3N_4−TCT−2AEDSEA. First, 1.5 g of graphene carbon nitride was dissolved in 25 mL of dry tetrahydrofuran. Then, 2 mmol of 2,4,6-trichloro-1,3,5-triazine (cyanuric chloride) was added to the mixture of reaction in an ice bath. The reaction was stirred for 3 h at 0−5 °C.[27] In the next step, 3 mmol of cystamine dihydrochloride and 6 mmol of triethylamine were dissolved in 10 mL of ethanol and slowly added to the reaction mixture. The mixture was stirred for 5 h at 80 °C; the obtained product was collected and washed with ethanol and distilled water (3 × 20 mL) and dried under ambient conditions (Scheme 1).

2.2.3. Preparation of Cu−Ni−Ag Nanoparticles. For the synthesis of Cu−Ni−Ag NPs, 1 mL solution of $NiCl_2{\cdot}6H_2O$ (0.5 M), 1 mL solution of $AgNO_3$ (0.5 M), and 1 mL solution of $CuCl_2{\cdot}2H_2O$ (0.5 M) were initially added to a volume of 20 mL of NaOH (5 M). After agitating the solution for 5 min, a volume of 0.35 mL of ethylenediamine was added to the solution, and agitation was uninterrupted for 1 h at room temperature. Then, 30 min after adding a volume of 0.3 mL of hydrazine hydrate (30%) to the mixture, it was transferred into a Teflon-lined autoclave made of stainless steel, which was stored in an oven for 4 h at 140 °C. An external magnet was used to collect the acquired black product, which was then rinsed three times using distilled water and ethanol (3 × 20 mL).[28]

2.2.4. Preparation of the g−C_3N_4−TCT−2AEDSEA−Ag−Cu−Ni Nanocomposite. The g−C_3N_4−TCT−2AEDSEA (1.0 g) and Cu−Ni−Ag NPs (0.5 g) were added to a volume of 30 mL of H_2O, and the mixture was subjected to ultrasound waves for 30 min. The reaction mixture underwent stirring at 40 °C for 12 h. As soon as the reaction was completed, an external magnet was used to collect the final catalyst, which was then rinsed three times using distilled water and ethanol (20 mL) and dried at 80 °C for 4 h.

https://doi.org/10.1021/acsomega.3c00572
ACS Omega 2023, 8, 18685−18694

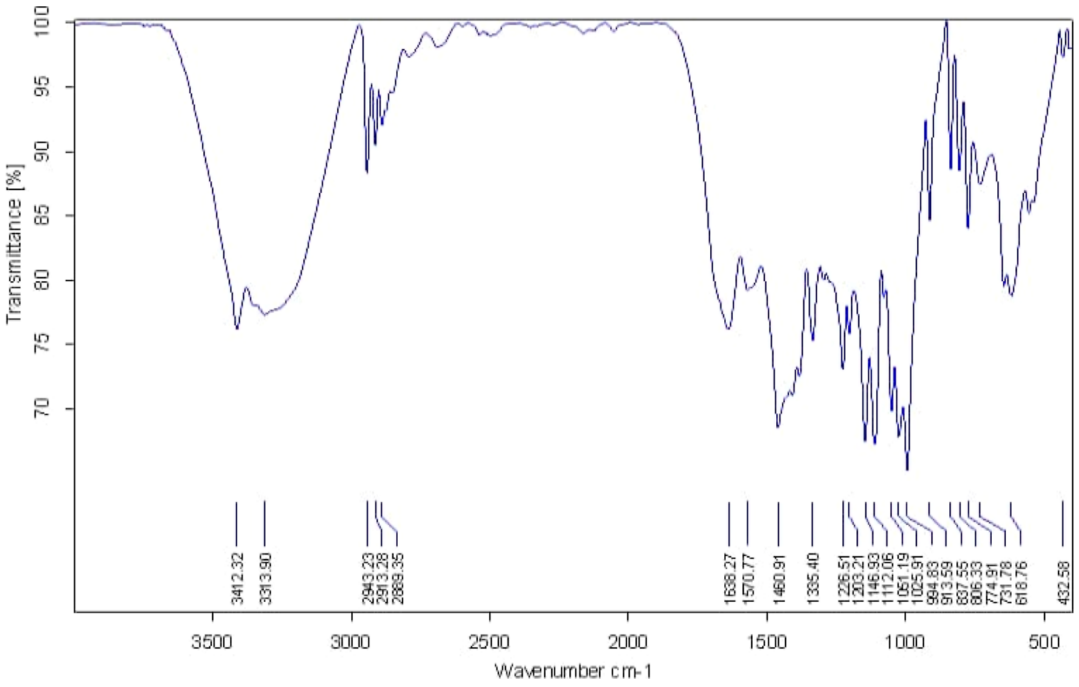

Figure 1. FT-IR spectra of g−C_3N_4−TCT−2AEDSEA.

2.3. General Method for the Synthesis of Propargylamine Derivatives via A^3-Coupling Reaction (a−k). In a sealed tube, aldehyde derivatives (1 mmol), morpholine (1.2 mmol), phenylacetylene (1.5 mmol), and the g−C_3N_4−TCT−2AEDSEA−Ag−Cu−Ni nanocomposite (20 mg) in 1 mL of toluene were added and heated at 80 °C for 8 h [checked by thin-layer chromatography (TLC)]. After the reaction was completed, the nanocomposite was isolated by an external magnet, and the products were purified with TLC plates (*n*-hexane/ethyl acetate 90:10). Eventually, all of the products were identified by ^{1}HNMR and ^{13}C NMR spectroscopy. The ^{1}H NMR and ^{13}C NMR spectra of all products are shown in the Supporting Information

2.3.1. 4-(1, 3-Diphenylprop-2-yn-1-yl) Morpholine (a). The product was obtained as a yellow oil. ^{1}H NMR (300 MHz, $CDCl_3$): δ (ppm): 7.73−7.39 (m, 10H, arom), 4.87 (s, 1H, CH−N), 3.81 (m, 4H, $2CH_2$−O), 2.72−2.70 (m, 4H, $2CH_2$−N).

^{13}C NMR (75 MHz, $CDCl_3$): δ (ppm): 137.7, 131.9, 128.7, 128.4, 128.3, 128.2, 127.9, 123.0, 88.6 (acetylenic carbon), 85.0 (acetylenic carbon), 67.2 (CH_2−O), 62.1 (CH_2−N), 49.9 (CH−N).

2.3.1.1. 4-(3-Phenyl-1-(p-tolyl) Prop-2-yn-1-yl) Morpholine (b). The product was obtained as a yellow oil. ^{1}H NMR (300 MHz, $CDCl_3$): δ (ppm): 7.59−7.37 (m, 7H, arom), 7.24 (d, J = 7.7 Hz, 2H, arom), 4.86 (s, 1H, CH−N), 3.83−3.78 (m, 4H, $2CH_2$−O), 2.74−2.71 (m, 4H, $2CH_2$−N), 2.41 (s, 3H, CH_3).

^{13}C NMR (75 MHz, $CDCl_3$): δ (ppm): 137.7, 134.3, 131.8, 129.0, 128.9, 128.7, 128.4, 122.9, 88.5 (acetylenic carbon), 85.0 (acetylenic carbon), 67.0 (CH_2−O), 61.9 (CH_2−N), 49.8 (CH−N), 21.2.

2.3.1.2. 4-(1-(4-Chlorophenyl)-3-phenylprop-2-yn-1-yl) Morpholine (c). The product was obtained as a yellow oil. ^{1}H NMR (300 MHz, $CDCl_3$): δ (ppm): 7.50 (d, J = 8.3 Hz, 2H, arom), 7.45−7.41 (m, 2H, arom), 7.27−7.24 (m, 5H, arom), 4.70 (s, 1H, CH−N), 3.68−3.65 (m, 4H, $2CH_2$−O), 2.56−2.53 (m, 4H, $2CH_2$−N).

^{13}C NMR (75 MHz, $CDCl_3$): δ (ppm): 136.3, 133.6, 131.8, 130.0, 128.5, 128.4, 128.3, 122.7, 89.0 (acetylenic carbon), 84.3 (acetylenic carbon), 67.1 (CH_2−O), 61.4 (CH_2−N), 49.8 (CH−N).

2.3.1.3. 4-(1-(2-Chlorophenyl)-3-phenylprop-2-yn-1-yl) Morpholine (d). The product was obtained as a yellow oil. ^{1}H NMR (300 MHz, $CDCl_3$): δ (ppm): 7.82−7.30 (m, 9H, arom), 5.19 (s, 1H, CH−N), 3.81−3.73 (m, 4H, $2CH_2$−O), 2.74−2.71 (m, 4H, $2CH_2$−N).

^{13}C NMR (75 MHz, $CDCl_3$): δ (ppm): 134.7, 131.8, 131.4, 130.6, 129.9, 129.2, 128.4, 128.3, 126.4, 122.8, 88.4 (acetylenic carbon), 84.7 (acetylenic carbon), 67.1 (CH_2−O), 59.0 (CH_2−N), 49.9 (CH−N).

2.3.1.4. 4-(1-(4-Bromophenyl)-3-phenylprop-2-yn-1-yl) Morpholine (e). The product was obtained as a yellow oil. ^{1}H NMR (300 MHz, $CDCl_3$): δ (ppm): 7.46−7.39 (m, 6H, arom), 7.28−7.24 (m, 3H, arom), 4.67 (s, 1H, CH−N), 3.67−3.63 (m, 4H, $2CH_2$−O), 2.55−2.52 (m, 4H, $2CH_2$−N).

^{13}C NMR (75 MHz, $CDCl_3$): δ (ppm): 136.9, 131.8, 131.4, 130.3, 128.5, 128.4, 122.7, 121.8, 89.0 (acetylenic carbon), 84.2 (acetylenic carbon), 67.1 (CH_2−O), 61.4 (CH_2−N), 49.8 (CH−N).

2.3.1.5. 4-(1-(2-Methoxyphenyl)-3-phenylprop-2-yn-1-yl) Morpholine (f). The product was obtained as a yellow oil. ^{1}H NMR (300 MHz, $CDCl_3$): δ (ppm): 7.70 (dd, J_1 = 7.5 Hz, J_2 = 1.8 Hz, 1H, arom), 7.54−7.51 (m, 2H, arom), 7.37−7.32 (m, 4H, arom), 7.04 (t, J = 7.2 Hz, 1H, arom), 6.97 (d, J = 8.2 Hz, 1H, arom), 5.26 (s, 1H, CH−N), 3.91 (s, 3H, O−CH_3), 3.80−3.76 (m, 4H, $2CH_2$−O), 2.79−2.70 (m, 4H, $2CH_2$−N).

^{13}C NMR (75 MHz, $CDCl_3$): δ (ppm): 157.2, 131.8, 130.3, 129.2, 128.3, 128.1, 125.8, 123.1, 120.3, 111.3, 86.7 (acetylenic carbon), 86.6 (acetylenic carbon), 67.1 (CH_2−O), 56.0 (O−CH_3), 55.0 (CH_2−N), 50.1 (CH−N).

2.3.1.6. 4-(1-(3-Fluorophenyl)-3-phenylprop-2-yn-1-yl) Morpholine (g). The product was obtained as a yellow oil. ^{1}H NMR (300 MHz, $CDCl_3$): δ (ppm): 7.59−7.55 (m, 2H, arom), 7.48 (t, J = 7.6 Hz, 2H, arom), 7.42−7.37 (m, 4H, arom), 7.05 (t,

https://doi.org/10.1021/acsomega.3c00572
ACS Omega 2023, 8, 18685−18694

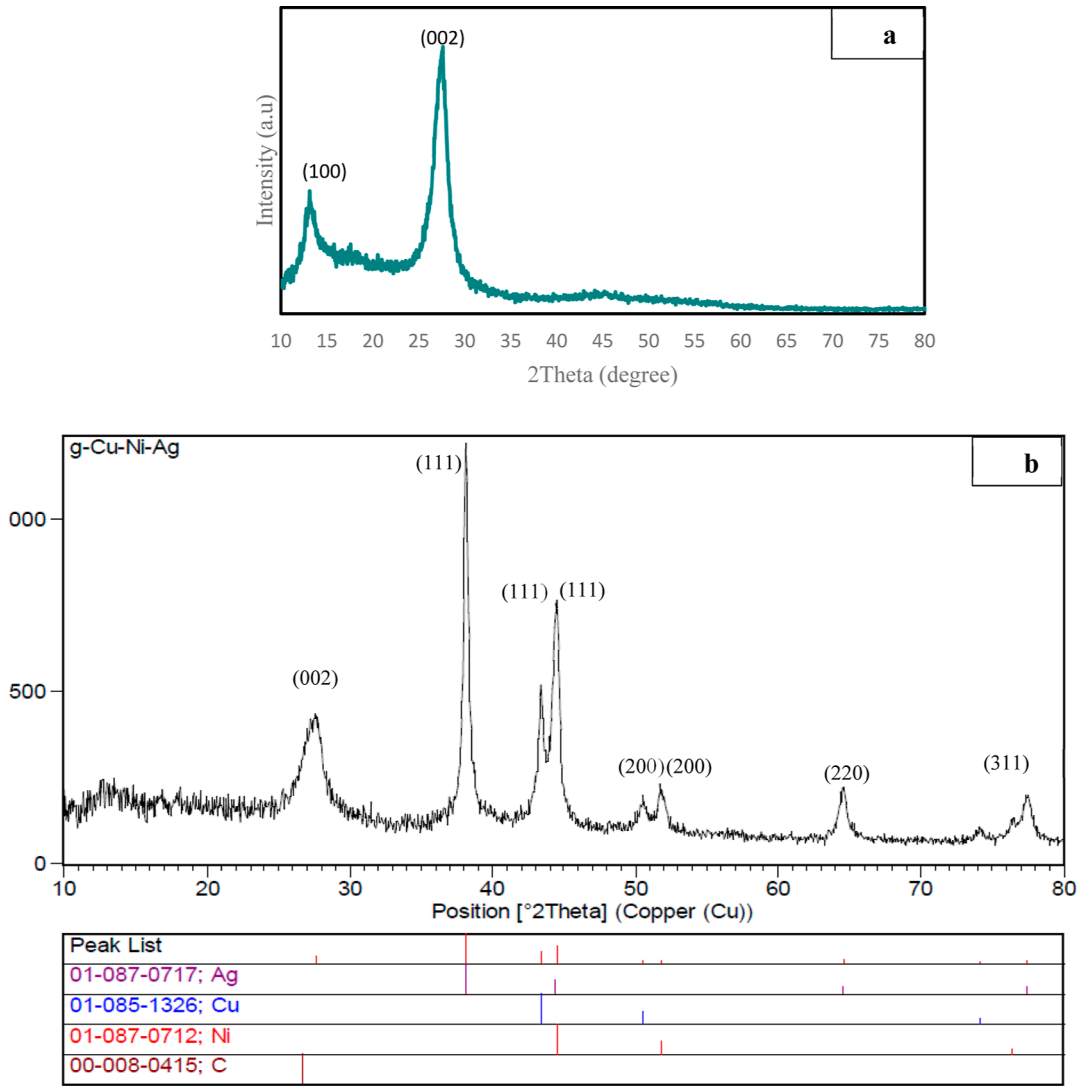

Figure 2. XRD patterns of (a) g−C_3N_4 and the (b) g−C_3N_4−TCT−2AEDSEA−Ag−Cu−Ni nanocomposite.

J = 7.2 Hz, 1H, arom), 4.85 (s, 1H, CH−N), 3.82−3.78 (m, 4H, $2CH_2$−O), 2.71−2.67 (m, 4H, $2CH_2$−N).

^{13}C NMR (75 MHz, $CDCl_3$): δ (ppm): 164.5, 161.3, 140.5, 131.9, 129.8, 129.6, 128.5, 128.4, 124.2, 124.1, 122.7, 115.6, 115.3, 114.9, 114.6, 89.0 (acetylenic carbon), 84.1 (acetylenic carbon), 67.1 (CH_2−O), 61.5 (CH_2−N), 49.8 (CH−N).

2.3.1.7. 4-(1-(2, 6-Dichlorophenyl)-3-phenylprop-2-yn-1-yl) Morpholine (h). The product was obtained as a yellow oil. ^{1}H NMR (300 MHz, $CDCl_3$): δ (ppm): 7.51−7.48 (m, 2H, arom), 7.40−7.33 (m, 5H, arom), 7.22 (t, J = 8.0 Hz, 1H, arom), 5.35 (s, 1H, CH−N), 3.77 (m, 4H, $2CH_2$−O), 2.97 (m, 2H, CH_2−N), 2.55 (m, 2H, CH_2−N).

^{13}C NMR (75 MHz, $CDCl_3$): δ (ppm): 136.5, 133.5, 131.8, 129.4, 129.3, 128.3, 128.2, 123.1, 86.8 (acetylenic carbon), 85.1 (acetylenic carbon), 67.1 (CH_2−O), 58.1 (CH_2−N), 51.3 (CH−N).

2.3.1.8. 4-(1-(4-Methoxyphenyl)-3-phenylprop-2-yn-1-yl) Morpholine (i). The product was obtained as a yellow oil. ^{1}H NMR (300 MHz, $CDCl_3$): δ (ppm): 7.62−7.56 (m, 4H, arom), 7.39−7.37 (m, 3H, arom), 6.96 (d, J = 8.7 Hz, 2H, arom), 4.82 (s, 1H, CH−N), 3.85 (s, 3H, O−CH_3), 3.82−3.78 (m, 4H, $2CH_2$−O), 2.71−2.69 (m, 4H, $2CH_2$−N).

^{13}C NMR (75 MHz, $CDCl_3$): δ (ppm): 159.3, 131.8, 129.8, 129.7, 128.4, 128.3, 123.0, 113.6, 88.4 (acetylenic carbon), 85.4 (acetylenic carbon), 67.1 (CH_2−O), 61.5 (O−CH_3), 55.3 (CH_2−N), 49.8 (CH−N).

2.3.1.9. 4-(1-(3-Chlorophenyl)-3-phenylprop-2-yn-1-yl) Morpholine (j). The product was obtained as a yellow oil. ^{1}H NMR (300 MHz, $CDCl_3$): δ (ppm): 7.56 (s, 1H, arom), 7.47−7.41 (m, 3H, arom), 7.26−7.20 (m, 5H, arom), 4.69 (s, 1H, CH−N), 3.68−3.60 (m, 4H, $2CH_2$−O), 2.56−2.53 (m, 4H, $2CH_2$−N).

^{13}C NMR (75 MHz, $CDCl_3$): δ (ppm): 140.0, 134.2, 131.9, 129.5, 128.6, 128.5, 128.4, 128.0, 126.7, 122.7, 89.1 (acetylenic carbon), 84.1 (acetylenic carbon), 67.1 (CH_2−O), 61.5 (CH_2−N), 49.8 (CH−N).

2.3.1.10. 4-(1-(2, 4-Dichlorophenyl)-3-phenylprop-2-yn-1-yl) Morpholine (k). The product was obtained as a yellow oil. ^{1}H NMR (300 MHz, $CDCl_3$): δ (ppm): 7.44−7.41 (m, 2H, arom), 7.37−7.36 (m, 1H, arom), 7.28−7.26 (m, 4H, arom), 7.19 (s, 1H, arom), 5.00 (s, 1H, CH−N), 3.64 (m, 4H, $2CH_2$−O), 2.59 (m, 4H, $2CH_2$−N).

^{13}C NMR (75 MHz, $CDCl_3$): δ (ppm): 135.3, 134.3, 131.8, 131.5, 131.3, 129.7, 128.5, 128.4, 126.7, 122.5, 88.7 (acetylenic

https://doi.org/10.1021/acsomega.3c00572
ACS Omega 2023, 8, 18685−18694

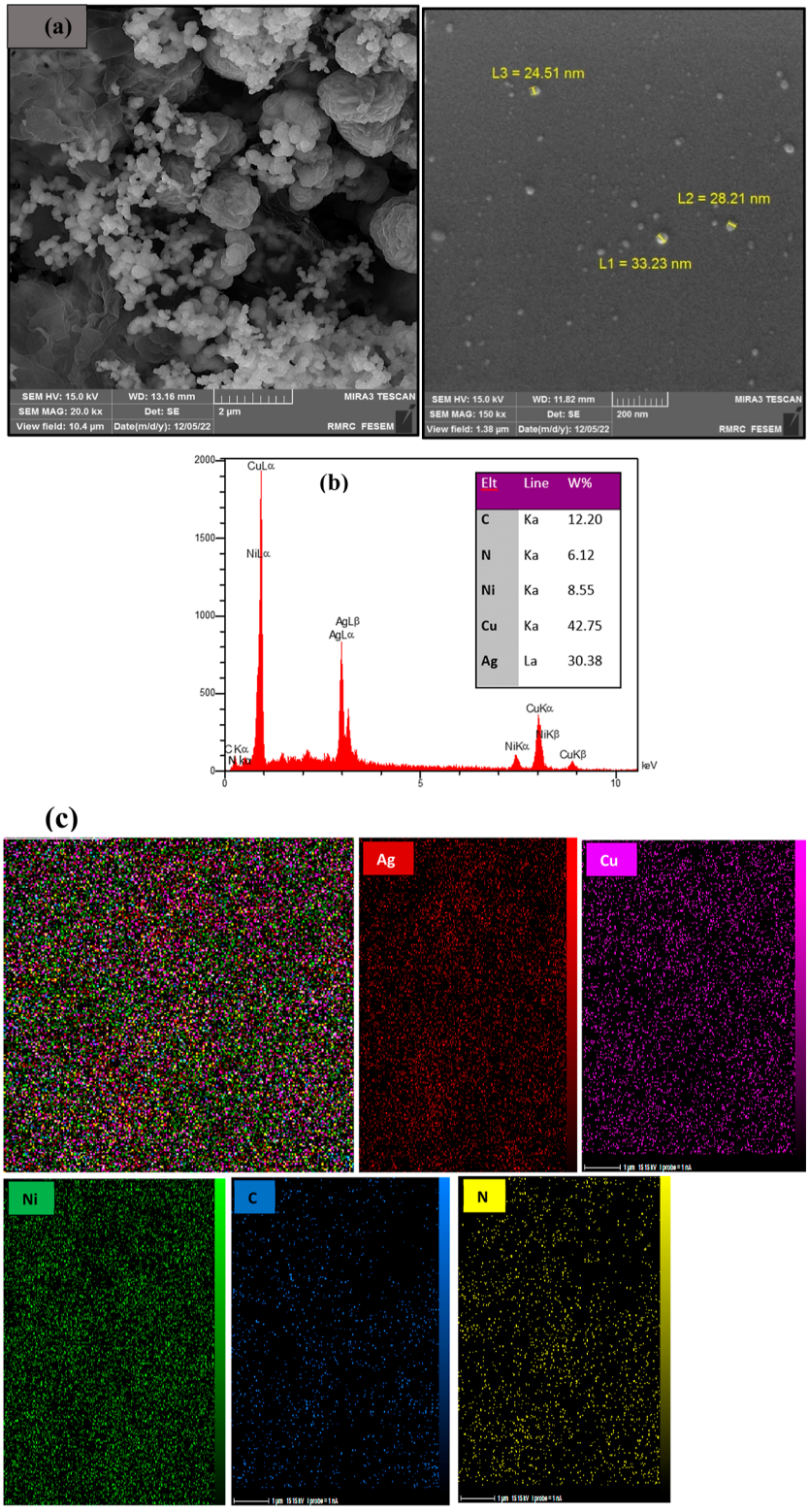

Figure 3. (a) FESEM images of the g−C_3N_4−TCT−2AEDSEA−Ag−Cu−Ni nanocomposite, (b) EDS spectrum, and (c) EDS mapping of the g−C_3N_4−TCT−2AEDSEA−Ag−Cu−Ni nanocomposite.

carbon), 84.0 (acetylenic carbon), 67.1 (CH_2−O), 58.6 (CH_2−N), 49.8 (CH−N).

3. RESULTS AND DISCUSSION

3.1. Characterization of the g−C_3N_4−TCT−2AEDSEA−Ag−Cu−Ni Nanocomposite. *3.1.1. Fourier-Transformed Infrared Spectroscopy.* By Fourier-transformed infrared (FT-IR) spectroscopy, the functional groups of g−C_3N_4−TCT−2AEDSEA can be appropriately analyzed and characterized. The g−C_3N_4−TCT−2AEDSEA FT-IR spectra are shown in Figure 1. The absorption peaks at 3314−3412 cm^{-1} are related to the vibration bending and stretching of N−H groups. The stretching

https://doi.org/10.1021/acsomega.3c00572
ACS Omega 2023, 8, 18685−18694

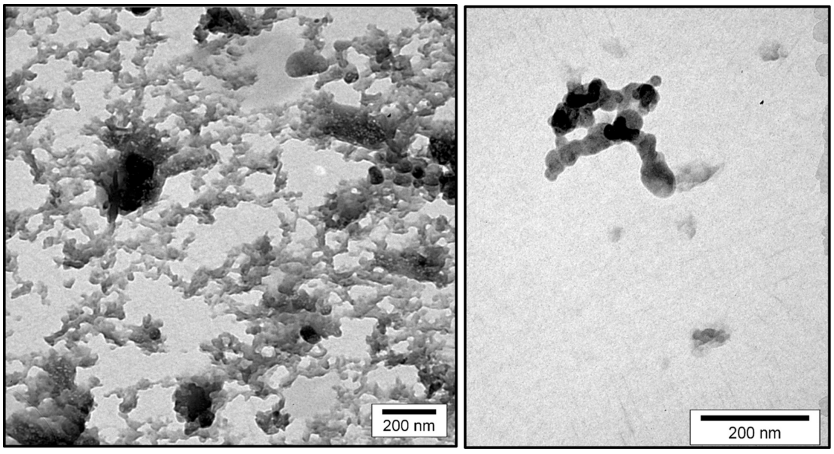

Figure 4. TEM of the g−C_3N_4−TCT−2AEDSEA−Ag−Cu−Ni nanocomposite.

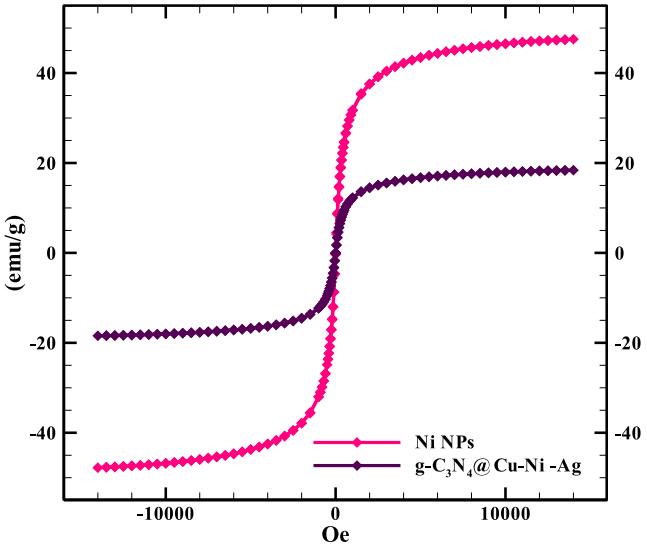

Figure 5. VSM analysis of Ni NPs and the g−C_3N_4−TCT−2AEDSEA−Ag−Cu−Ni nanocomposite.

and bending vibrations of the C−H group of cystamine dihydrochloride appeared at 2889−2943 and 1460 cm^{-1}, respectively. The band appearing at 1638 cm^{-1} can be ascribed to the vibrations of the C═N groups. Moreover, the small band that appeared at 432 cm^{-1} belongs to vibrations of the S−S bond.

3.1.2. XRD Analysis. The XRD pattern of g−C_3N_4 and the g−C_3N_4−TCT−2AEDSEA−Ag−Cu−Ni nanocomposite is shown in Figure 2a. The pure g−C_3N_4 exhibits two peaks at 2θ = 13.1 and 27.5°, which are assigned to the (100) and (002) planes (Figure 2a). The peaks related to the g−C_3N_4−TCT−2AEDSEA−Ag−Cu−Ni appeared at 2θ = 27.76, 38.14, 43.35, 50.46, 51.79, 64.61, and 77.43° which can be corresponding to the (002), (111),(111), (111), (200), (200), (220), and (311) planes (Figure 2b). Then, the Debye−Scherrer equation was used to calculate the average size of crystallites/grains, in which λ stands for the X-ray wavelength, k symbolizes the Scherrer coefficient, θ stands for the diffraction angle, β is the full width at half-maximum intensity, and D denotes the average crystal size (eq 1). The approximate average size of crystallites of copper and nickel nanoparticles was 44.71 nm.

Table 1. Optimization of Reaction Conditions for the Synthesis of Propargylamines[a]

entry	catalyst(mg)	solvent	T (°C)	time (h)	yield[b] (%)
1	20	EtOH	100	10	trace
2	20	H_2O	75	10	10
3	20	DMF	100	10	65
4	20	toluene	100	10	80
5	20	dioxane	80	10	46
6	20	toluene	100	10	68
7	20	toluene	100	10	50
8	20	toluene	80	10	87
9	20	toluene	60	10	73
10	20	toluene	25	10	0
11	20	toluene	80	8	90[c]
12	20	toluene	80	6	61
13	30	toluene	80	8	86
14	10	toluene	80	8	53
15		toluene	80	8	0

[a]Reaction conditions: benzaldehyde (1.0 mmol), morpholine (1.2 mmol), phenylacetylene (1.5 mmol), catalyst, 1 mL of solvent. [b]Isolated yield. [c]Optimized conditions.

Scheme 2. General Reaction for the Synthesis of Propargylamine Derivatives

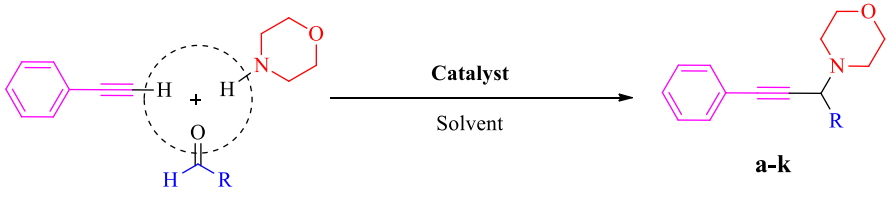

Catalyst: g-C_3N_4-TCT-2AEDSEA -Ag-Cu-Ni nanocomposite

https://doi.org/10.1021/acsomega.3c00572
ACS Omega 2023, 8, 18685−18694

Table 2. A^3-Coupling of Aldehyde Derivatives, Morpholine, and Phenylacetylene Catalyzed by the g−C_3N_4−TCT−2AEDSEA−Ag−Cu−Ni Nanocomposite[a]

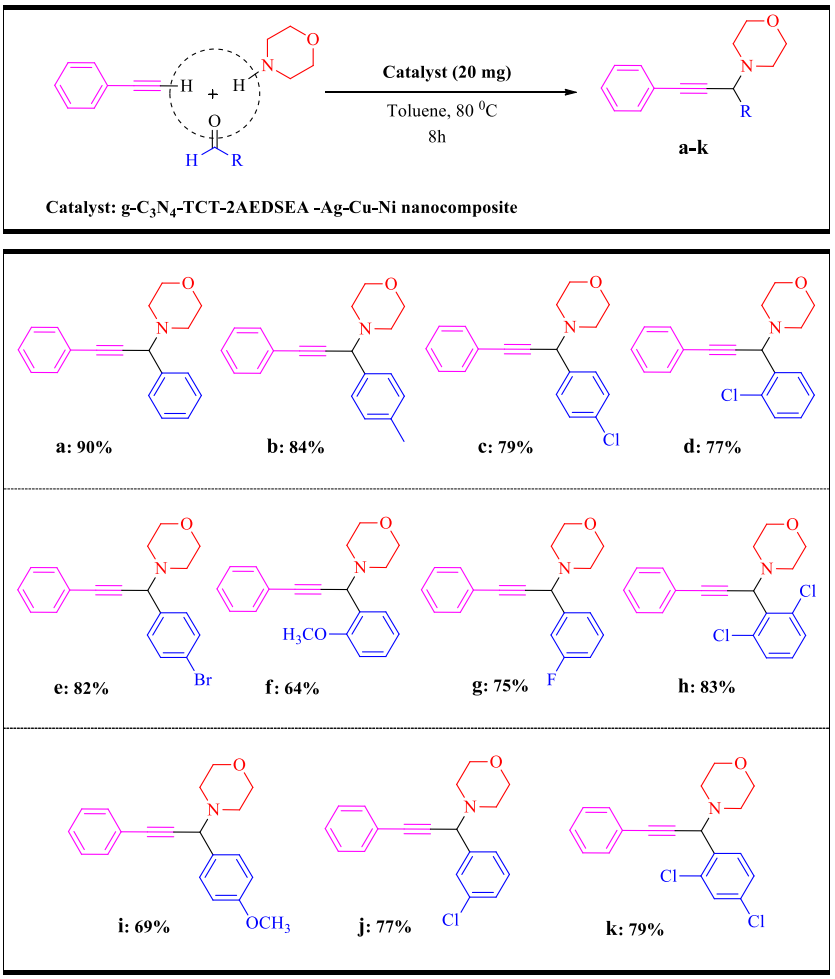

[a]Reaction conditions: Aldehyde (1.0 mmol), secondary amine(1.2 mmol), phenylacetylene (1.5 mmol), toluene (1 mL) in the presence of the nanocomposite (20 mg) at 80 °C for 8 h.

Scheme 3. Suggested Mechanism for the A^3-Coupling Reaction

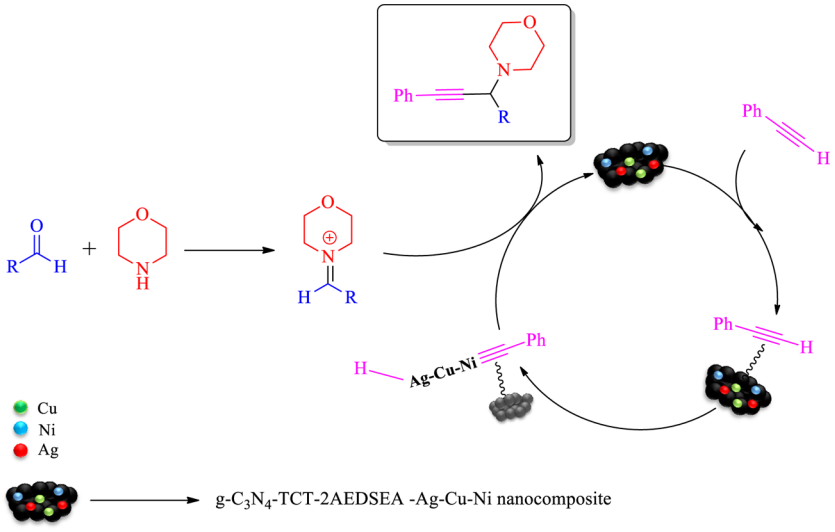

$$D = \frac{k\lambda}{\beta}\cos\theta \quad (1)$$

3.1.3. FESEM Images and EDS Analysis. Field-emission scanning electron microscopy images of the g−C_3N_4−TCT−2AEDSEA−Ag−Cu−Ni nanocomposite are shown in Figure 3a.

https://doi.org/10.1021/acsomega.3c00572
ACS Omega 2023, 8, 18685−18694

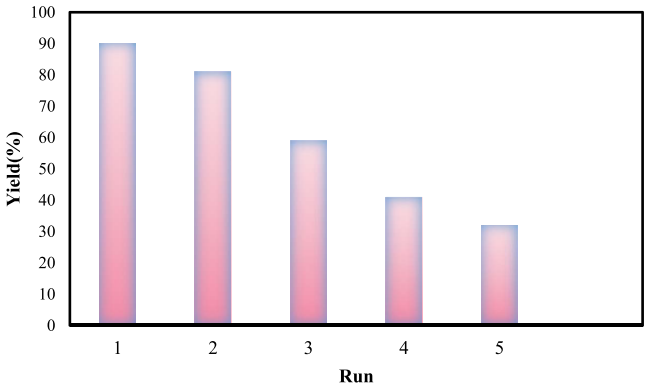

Figure 6. Reusability of the g−C_3N_4−TCT−2AEDSEA−Ag−Cu−Ni nanocomposite in the synthesis of compound a.

As can be seen, the morphology of the Ag−Cu−Ni NPS was quasi-spherical, and they were decorated on the surface of g−C_3N_4−TCT−2AEDSEA, indicating the successful synthesis of the g−C_3N_4−TCT−2AEDSEA−Ag−Cu−Ni nanocomposite. To further confirm the presence of Ag−Cu−Ni NPs, energy-dispersive X-ray spectroscopy (EDS) and EDS mapping were carried out and are shown in Figure 3b,c. The result shows the presence of nitrogen, carbon, Ag, Cu, and Ni atoms in the nanocomposite.

3.1.4. TEM Images of the g−C_3N_4−TCT−2AEDSEA−Ag−Cu−Ni Nanocomposite. TEM images of the prepared nanocomposite are shown in Figure 4. These images show that most of the particles with a quasi-spherical morphology were located on the surface of g−C_3N_4−TCT−2AEDSEA. In addition, the TEM images of the catalyst demonstrate that the nanoparticles are dispersed in the composite matrix.

3.1.5. Magnetic Property. Figure 5 shows the magnetic features of the nanocomposite at room temperature organized to utilize a vibrating sample magnetometer. The magnetic saturation values were obtained at 47.52 for Ni NPs and 18.39 emu g^{-1} for the g−C_3N_4−TCT−2AEDSEA−Ag−Cu−Ni nanocomposite. A slight decrease in the saturation magnetization values of Ni NPs was observed after loading nanoparticles on the surface of g−C_3N_4−TCT−2AEDSEA. The reason for this decrease is the existence of non-magnetic g−C_3N_4−TCT−2AEDSEA (Figure 5). In fact, this material has a protective effect on Ni NPs. This reduction, however, did not prevent the absorption of the nanocatalyst by the external magnet.

3.2. Catalytic Activity of the g−C_3N_4−TCT−2AEDSEA−Ag−Cu−Ni Nanocomposite in the A^3-Coupling Reaction. After characterization, the catalytic activity of the g−C_3N_4−TCT−2AEDSEA−Ag−Cu−Ni nanocomposite as a catalyst was studied in the A^3-coupling reaction for the synthesis of propargylamines (Scheme 2).

In an endeavor to obtain improved yields, first, the reaction between benzaldehyde, morpholine, and phenylacetylene in the presence of synthesized nanocomposite under various conditions was studied to set up the optimal conditions. The results are shown in Table 1. For this purpose, we have selected the reaction of benzaldehyde (1.0 mmol), morpholine (1.2 mmol), and phenylacetylene (1.5 mmol) in the presence of 20 mg of the nanocomposite in 1 mL of solvent as a model to consider for the synthesis of compound a. First, this reaction was carried out in the presence of various solvents such as EtOH, H_2O, DMF, toluene, and dioxane and 20 mg of catalyst for 10 h (Table 1, entries 1−5). As can be seen, the toluene solvent showed more suitable efficiency. The amount of catalyst was also optimized; increasing and decreasing the amount of catalyst up to 30 and 10 mg did not significantly increase the efficiency (Table 1, entries 13−14). The results show that this reaction performs better in the presence of 20 mg of catalyst. This reaction was also accomplished at different temperatures, and the highest efficiency was observed at 80 °C (Table 1, entries 8−10). Optimization of the reaction time indicated that this reaction is completed in the presence of the g−C_3N_4−TCT−2AEDSEA−Ag−Cu−Ni nanocomposite in 8 h with the most increased efficiency (Table 1, entry 11). As anticipated, no product formation can be observed in the absence of the catalyst (Table 1, entry 15). Eventually, the amount of 20 mg of catalyst and toluene as the reaction solvent at 80 °C for 8 h was selected as optimal conditions (Table 1, entry 11).

Then, different aldehydes were subjected to optimal conditions to evaluate the effect of different substituents on the reaction efficiency. The results are listed in Table 2. All the products were purified using TLC. In addition to confirming their physical properties with previously reported values, the structure of these compounds was also confirmed by ^{1}H NMR and ^{13}C NMR spectroscopy. In the ^{1}H NMR spectrum of compound b, the C−H proton was seen as a singlet at δ = 4.86 ppm. The CH_3 protons were seen as a singlet at δ = 2.41 ppm. Protons of morpholine and the aromatic ring appeared at 2.74−2.71 ($2CH_2$−N) and 3.83−3.78 ($2CH_2$−O) ppm and 7.59−7.23 ppm, respectively. The ^{13}C NMR spectrum exhibited 14 signals that are consistent with the proposed structure. Two peaks in areas 88.5 and 85.0 ppm indicate the presence of acetylenic carbons.t Also, the CH_3 group was observed at 21.2 ppm.

3.3. Mechanism Presented for the A^3-Coupling Reaction. Scheme 3 illustrates the presented mechanism of the A^3-coupling reaction between amine, phenylacetylene, and aldehyde. Initially, the nanocomposite activates phenylacetylene. Eventually, with the addition of the acetyl complex to the immonium ion, which consists of the reaction between the aldehyde and the amine, the final product was obtained.

Table 3. Comparisons of the g−C_3N_4−TCT−2AEDSEA−Ag−Cu−Ni Nanocomposite with Some Previously Reported Catalysts for the Synthesis of Compound a

entry	catalyst	reaction conditions	time (h)	yield (%)	[ref]
1	Au@CS_2−AP@Fe_3O_4	H_2O/90 °C	24	86	[29
2	AgTPA (tungstophosphoric acid)	acetonitrile/80 °C	5	80	[30
3	Biochar@Cu−Ni	toluene/80 °C	8	80	[31
4	Fe_3O_4@T-CS@Cys@Ag^+	CH_3CN	1	95	[32
5	Fe_3O_4@R.tinctorum/Ag NPs	toluene/80 °C	48	96	[33
6	g−C_3N_4−TCT−2AEDSEA−Ag−Cu−Ni	toluene/80°C	8	91	this work

https://doi.org/10.1021/acsomega.3c00572
ACS Omega 2023, 8, 18685−18694

3.4. Recyclability of the g−C_3N_4−TCT−2AEDSEA−Ag−Cu−Ni Nanocomposite in the A^3-Coupling Reaction. Finally, the recyclability of the nanocomposites of g−C_3N_4−TCT−2AEDSEA−Ag−Cu−Ni was studied in the model reaction subject to the optimized circumstances. Upon completing the first run of the reaction, an external magnet was used to separate the catalyst from the reaction mixture, which was then rinsed twice using water and ethanol (2 × 10) in order to remove the overall potential impurity remnants from the nanocomposite surface. The reaction was repeated for five successive runs. The decrease observed in the recovery efficiency of nanocomposite can be attributed to Ag−Cu−Ni NPs' loss during the recycling process. Figure 6 exhibits the results of the recyclability of the nanocomposite after recycling 5 times.

The efficacy of the g−C_3N_4−TCT−2AEDSEA−Ag−Cu−Ni nanocomposite was compared with that of some previously reported catalysts for compound a (Table 3). Short reaction time, high yield, ease of catalyst separation, and reusability are the advantages of the synthesized catalyst.

4. CONCLUSIONS

In order to create active centers for nanoparticle attachment, the surface of g−C_3N_4 was functionalized by organic functional groups such as melamine and cystamine dihydrochloride. In this study, Ag−Cu−Ni nanoparticles were synthesized using hydrazine hydrate as the reducing agent and ethylenediamine as the capping agent. The catalytic activity of the g−C_3N_4−TCT−2AEDSEA−Ag−Cu−Ni nanocomposite was examined in an A^3-coupling reaction to synthesize propargylamine derivatives. The synthesized nanocomposite showed high performance in the synthesis of propargylamines through the A^3-coupling reaction in toluene as a solvent. The advantages of the nanocomposite include easy separation through an external magnet and its reusability. To the best of our knowledge, there are few studies on locating the Ag−Cu−Ni nanoparticles on the surface of functionalized g−C_3N_4 for the A^3-coupling reaction..

■ ASSOCIATED CONTENT

Supporting Information

The Supporting Information is available free of charge at https://pubs.acs.org/doi/10.1021/acsomega.3c00572.

^{1}HNMR and ^{13}C NMR spectra of all products (PDF)

■ AUTHOR INFORMATION

Corresponding Author

Hassan Sheibani − *Department of Chemistry, Shahid Bahonar University of Kerman, Kerman 76169, Iran;* orcid.org/0000-0001-5971-4567; Email: ahsheibani@uk.ac.ir

Authors

Mohammad Zarei − *Department of Chemistry, Shahid Bahonar University of Kerman, Kerman 76169, Iran*

Iman Mohammadzadeh − *Endodontology Research Center, Kerman University of Medical Sciences, Kerman 76188, Iran; Social Determinants on Oral Health Research Center, Kerman University of Medical Sciences, Kerman 76188, Iran*

Kazem Saidi − *Department of Chemistry, Shahid Bahonar University of Kerman, Kerman 76169, Iran*

Complete contact information is available at: https://pubs.acs.org/10.1021/acsomega.3c00572

Notes

The authors declare no competing financial interest.

■ ACKNOWLEDGMENTS

The authors express appreciation to the Shahid Bahonar University of Kerman Faculty Research Committee Fund for its support of this investigation.

■ REFERENCES

(1) Sheldon, R. A. E. E factors, green chemistry and catalysis: an odyssey. *Chemical Communications* **2008**, 3352−3365.

(2) Sheldon, R. A. Fundamentals of green chemistry: efficiency in reaction design. *Chem. Soc. Rev.* **2012**, *41*, 1437−1451.

(3) Karimi, B.; Gholinejad, M.; Khorasani, M. Highly efficient three-component coupling reaction catalyzed by gold nanoparticles supported on periodic mesoporous organosilica with ionic liquid framework. *Chemical communications* **2012**, *48*, 8961−8963.

(4) Kakuchi, R. The dawn of polymer chemistry based on multicomponent reactions. *Polymer Journal* **2019**, *51*, 945−953.

(5) Jones, J.; Lu, S. Y.; Shevchenko, V.; Nagaev, I. Y.; Myasoedov, N.; Susan, A.; Anderskerskevitz, R.; Birke, F.; Switek, K. H.; Wiegerinck, P.; et al. 10th Conference of the Central European Division eV of the International Isotope Society. *Journal of Labelled Compounds and Radiopharmaceuticals: The Official Journal of the International Isotope Society* **2002**, *45*, 1159−1198.

(6) Oliver Kappe, C. 100 years of the Biginelli dihydropyrimidine synthesis. *Tetrahedron* **1993**, *49*, 6937−6963.

(7) Arend, M.; Westermann, B.; Risch, N. Moderne Varianten der Mannich-Reaktion. *Angew. Chem.* **1998**, *110*, 1096−1122.

(8) Ugi, I.; Dömling, A.; Hörl, W. Multicomponent reactions in organic chemistry. *Endeavour* **1994**, *18*, 115−122.

(9) Wei, C.; Li, Z.; Li, C.-J. The development of A3-coupling (aldehyde-alkyne-amine) and AA3-coupling (asymmetric aldehyde-alkyne-amine). *Synlett* **2004**, *35*, 1472−1483.

(10) Traverse, J. F.; Hoveyda, A. H.; Snapper, M. L. Enantioselective synthesis of propargylamines through Zr-catalyzed addition of mixed alkynylzinc reagents to arylimines. *Org. Lett.* **2003**, *5*, 3273−3275.

(11) Prajapati, D.; Laskar, D. D.; Gogoi, B. J.; Devi, G. Indium-mediated propargylation of imines and imine oxides in aqueous media: propargylation of >C═N-centres. *Tetrahedron letters* **2003**, *44*, 6755−6757.

(12) Peshkov, V. A.; Pereshivko, O. P.; Van der Eycken, E. V. A walk around the A 3-coupling. *Chem. Soc. Rev.* **2012**, *41*, 3790−3807.

(13) Lauder, K.; Toscani, A.; Scalacci, N.; Castagnolo, D. Synthesis and reactivity of propargylamines in organic chemistry. *Chemical reviews* **2017**, *117*, 14091−14200.

(14) Liu, Y. Recent advances on diversity-oriented heterocycle synthesis via multicomponent tandem reactions based on A3-coupling. *Arkivoc* **2013**, *2014*, 1−20.

(15) Vessally, E.; Hosseinian, A.; Edjlali, L.; Bekhradnia, A.; Esrafili, M. D. New page to access pyridine derivatives: synthesis from N-propargylamines. *RSC advances* **2016**, *6*, 71662−71675.

(16) Matsuda, I.; Sakakibara, J.; Nagashima, H. A Novel Approach to α-Silylmethylene-β-lactams via Rh-catalyzed Silylcarbonylation of Propargylamine Derivatives. *Tetrahedron letters* **1991**, *32*, 7431−7434.

(17) Shi, L.; Tu, Y.-Q.; Wang, M.; Zhang, F.-M.; Fan, C.-A. Microwave-promoted three-component coupling of aldehyde, alkyne, and amine via C− H activation catalyzed by copper in water. *Org. Lett.* **2004**, *6*, 1001−1003.

(18) Wei, C.; Li, C.-J. A highly efficient three-component coupling of aldehyde, alkyne, and amines via C− H activation catalyzed by gold in water. *J. Am. Chem. Soc.* **2003**, *125*, 9584−9585.

(19) Yan, W.; Wang, R.; Xu, Z.; Xu, J.; Lin, L.; Shen, Z.; Zhou, Y. A novel, practical and green synthesis of Ag nanoparticles catalyst and its application in three-component coupling of aldehyde, alkyne, and amine. *J. Mol. Catal. A: Chem.* **2006**, *255*, 81−85.

(20) Ramu, E.; Varala, R.; Sreelatha, N.; Adapa, S. R. Zn (OAc) 2· 2H2O: a versatile catalyst for the one-pot synthesis of propargylamines. *Tetrahedron Lett.* **2007**, *48*, 7184−7190.
(21) Fischer, C.; Carreira, E. M. Direct addition of TMS-acetylene to aldimines catalyzed by a simple, commercially available Ir (I) complex. *Org. Lett.* **2001**, *3*, 4319−4321.
(22) Veisi, H.; Taheri, S.; Hemmati, S. Preparation of polydopamine sulfamic acid-functionalized magnetic Fe 3 O 4 nanoparticles with a core/shell nanostructure as heterogeneous and recyclable nanocatalysts for the acetylation of alcohols, phenols, amines and thiols under solvent-free conditions. *Green Chem.* **2016**, *18*, 6337−6348.
(23) Veisi, H.; Dadres, N.; Mohammadi, P.; Hemmati, S. Green synthesis of silver nanoparticles based on oil-water interface method with essential oil of orange peel and its application as nanocatalyst for A3 coupling. *Materials Science and Engineering: C* **2019**, *105*, 110031.
(24) Ekka, B.; Dhar, G.; Sahu, S.; Mishra, M.; Dash, P.; Patel, R. K. Removal of Cr (VI) by silica-titania core-shell nanocomposites: In vivo toxicity assessment of the adsorbent by Drosophila melanogaster. *Ceram. Int.* **2021**, *47*, 19079−19089.
(25) Sahu, S.; Bishoyi, N.; Sahu, M. K.; Patel, R. K. Investigating the selectivity and interference behavior for detoxification of Cr (VI) using lanthanum phosphate polyaniline nanocomposite via adsorption-reduction mechanism. *Chemosphere* **2021**, *278*, 130507.
(26) Zarei, M.; Mohammadzadeh, I.; Saidi, K.; Sheibani, H. g-C3N4 quantum dot decorated MoS2/Fe3O4 as a novel recoverable catalyst for photodegradation of organic pollutant under visible light. *J. Mater. Sci.: Mater. Electron.* **2021**, *32*, 26213−26231.
(27) Mohammadi, P.; Heravi, M. M.; Sadjadi, S. Green synthesis of Ag NPs on magnetic polyallylamine decorated g-C3N4 by Heracleum persicum extract: efficient catalyst for reduction of dyes. *Scientific reports* **2020**, *10*, 6579.
(28) Zarei, M.; Mohammadzadeh, I.; Saidi, K.; Sheibani, H. Fabrication of biochar@ Cu-Ni nanocatalyst for reduction of aryl aldehyde and nitroarene compounds. *Biomass Conversion and Biorefinery* **2022**, 1−16.
(29) Loni, M.; Yazdani, H.; Bazgir, A. Gold nanoparticles-decorated dithiocarbamate nanocomposite: an efficient heterogeneous catalyst for the green A3-coupling synthesis of propargylamines. *Catal. Lett.* **2018**, *148*, 3467−3476.
(30) Mohan Reddy, K.; Seshu Babu, N.; Suryanarayana, I.; Sai Prasad, P.; Lingaiah, N. The silver salt of 12-tungstophosphoric acid: an efficient catalyst for the three-component coupling of an aldehyde, an amine and an alkyne. *Tetrahedron letters* **2006**, *47*, 7563−7566.
(31) Zarei, M.; Saidi, K.; Sheibani, H. Preparation and investigation of catalytic activities of Cu-Ni nanoparticles supported on the biochar derived from pomegranate shells in the A3-coupling reactions. *Biomass Conversion and Biorefinery* **2022**, 1−13.
(32) Rafiee, F.; Hosseinvand, S. KA2 and A3 coupling reactions promoted by Fe3O4@ T-CS@ Cys@ Ag+ nanocomposite. *Polymer Bulletin* **2022**, *79*, 2799−2817.
(33) Veisi, H.; Mohammadi, L.; Hemmati, S.; Tamoradi, T.; Mohammadi, P. In situ immobilized silver nanoparticles on rubia tinctorum extract-coated ultrasmall iron oxide nanoparticles: an efficient nanocatalyst with magnetic recyclability for synthesis of propargylamines by A3 coupling reaction. *ACS omega* **2019**, *4*, 13991−14003.

https://doi.org/10.1021/acsomega.3c00572
ACS Omega 2023, 8, 18685−18694